

# Synthesis and Isomerisation Reactions of Tetranuclear and Octanuclear (Carbamato)zinc Complexes

Peter F. Haywood,<sup>[a]</sup> Matthew R. Hill,<sup>[b]</sup> Nicholas K. Roberts,<sup>[a]</sup> Donald C. Craig,<sup>[a]</sup> Jennifer J. Russell,<sup>[c]</sup> and Robert N. Lamb\*<sup>[d]</sup>

**Keywords:** Carbamato ligands / Chemical vapor deposition / Dialkylcarbamates / Isomerisation / Oxido ligands / Zinc

A new series of (diisopropylcarbamato)(oxido)zinc complexes were obtained by innovative synthetic approaches. The (carbamato)zinc clusters  $[\text{Zn}_4(\mu_4\text{-O})(\text{O}_2\text{CNiPr}_2)_6]$  (**1**) and  $[\text{Zn}_8(\mu_4\text{-O})_2(\text{O}_2\text{CNiPr}_2)_{12}]$  (**2**) were synthesised by an identical reaction procedure involving protolysis of  $\text{ZnEt}_2$  with  $i\text{Pr}_2\text{NH}/\text{CO}_2$  and followed by stoichiometric hydrolysis. Recrystallisation of the reaction product from nitrile solvents yielded the tetrazinc complex **1**. Conversely, recrystallisation from alkane solvents yielded crystals of the octazinc complex **2**. The two structural isomers were readily interconverted simply by recrystallisation from the appropriate solvent. Both complexes were structurally characterised by X-ray crystallogra-

phy. The tetrazinc complex **1** has the quintessential basic zinc acetate type structure. Its dimer, the octazinc complex **2** is a new derivative of the  $[\text{M}_8(\mu_4\text{-O})_2(\text{O}_2\text{CNiPr}_2)_{12}]$  class, examples of which are known for all other first-row transition metals. The solution chemistry was investigated using variable-temperature NMR spectroscopy and ESI-MS. The new synthetic approach offers a route to other similar complexes. Thus, using  $\text{Et}_2\text{NH}$  in place of  $i\text{Pr}_2\text{NH}$  yielded the known complex  $[\text{Zn}_4(\mu_4\text{-O})(\text{O}_2\text{CNEt}_2)_6]$  (**3**).

(© Wiley-VCH Verlag GmbH & Co. KGaA, 69451 Weinheim, Germany, 2008)

## Introduction

The tetrahedral  $[\text{Zn}_4\text{O}]^{6+}$  core is a common motif in zinc coordination chemistry with examples among the zinc carboxylates,<sup>[1,2]</sup> carbamates<sup>[3–6]</sup> and phosphates.<sup>[7,8]</sup> In the carboxylato and carbamato series, this core is extended by bridging oxygen atoms into a framework reminiscent of wurtzite-type  $\text{ZnO}$ .<sup>[9]</sup> It is for this reason that the carbamato complex  $[\text{Zn}_4(\mu_4\text{-O})(\text{O}_2\text{CNEt}_2)_6]$ <sup>[3]</sup> has been described as “a further molecular model of crystalline  $\text{ZnO}$ ”.<sup>[10]</sup>

Recent studies<sup>[6,11]</sup> on  $[\text{Zn}_4(\mu_4\text{-O})(\text{O}_2\text{CNEt}_2)_6]$  and similar complexes showed that the  $[\text{Zn}_4\text{O}]^{6+}$  core has a remarkable effect on the reactivity of carbamato ligands, both the carboxylic and amino components possessing intrinsic lability not ordinarily observed in organic carbamates. The  $[\text{Zn}_4(\mu_4\text{-O})(\text{O}_2\text{CNEt}_2)_6]$  complex and its chemical properties are of interest to us from an electronics perspective: in 2002,

we showed<sup>[12]</sup> that  $[\text{Zn}_4(\mu_4\text{-O})(\text{O}_2\text{CNEt}_2)_6]$  is volatile under high vacuum and can be used to deposit *c*-axis-oriented polycrystalline  $\text{ZnO}$  films by the single-source chemical vapour deposition (SSCVD) process. SSCVD is an unusual deposition technique in that it requires no gas-phase mixing of separate reagents. Instead, it relies on all the desired film constituents being packaged within a specifically designed volatile “precursor” molecule. This technique has been described previously.<sup>[13]</sup> In our SSCVD depositions of  $\text{ZnO}$ , we have used zinc carboxylates,<sup>[13,14]</sup> zinc  $\beta$ -diketonates and zinc oximates<sup>[15]</sup> as precursors. However, ideal single-source behaviour was only observed with the (carbamato)zinc complex  $[\text{Zn}_4(\mu_4\text{-O})(\text{O}_2\text{CNEt}_2)_6]$ ,<sup>[12]</sup> as the other precursors required additional oxygen sources to suppress the formation of high-carbon amorphous  $\text{ZnO}$ .<sup>[16]</sup> This singular behaviour of  $[\text{Zn}_4(\mu_4\text{-O})(\text{O}_2\text{CNEt}_2)_6]$  may be due to the lability of the C–N bond of the diethylcarbamato ligand,<sup>[11]</sup> which may permit a facile decomposition pathway not available in the other complexes.

The advantage that lability of the C–N bond gives to the  $\text{ZnO}$  deposition process brings with it stability problems. The sensitivity of carbamates to hydrolysis is well known,<sup>[17]</sup> with loss of  $\text{CO}_2$  being the thermodynamic driving force. The modest stability of  $[\text{Zn}_4(\mu_4\text{-O})(\text{O}_2\text{CNEt}_2)_6]$  makes it less than ideal as an SSCVD precursor. We found that, for a given sample, its utility for film deposition deteriorated over a period of 2 weeks, even when stored under inert conditions. Moreover, its temperature sensitivity leads to sig-

[a] School of Chemistry, University of New South Wales, Sydney NSW 2052, Australia

[b] Commonwealth Scientific and Industrial Research Organisation, Division of Materials Science and Engineering, Private Bag 33, Clayton South MDC Victoria, 3169 Australia

[c] School of Materials Science, University of New South Wales, Sydney NSW 2052, Australia

[d] School of Chemistry, University of Melbourne, Victoria, 3010 Australia  
Fax: +61-3-9347-5180

E-mail: rnlamb@unimelb.edu.au

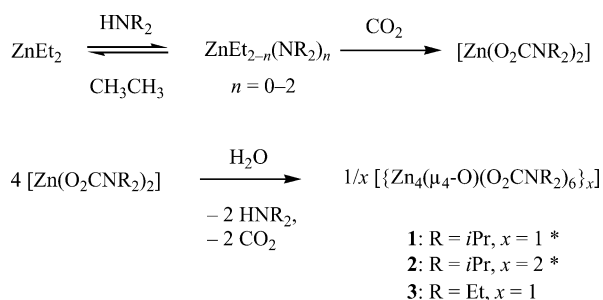
Supporting information for this article is available on the WWW under <http://www.eurjic.org> or from the author.

nificant premature decomposition in the Knudsen cell during SSCVD depositions, so that the accompanying outgassing and intra-cell deposition of oxides affects the vapour pressure profile of the precursor, thereby affecting the reproducibility of the deposition.

With this problem in mind, we sought to develop analogous (dialkylcarbamato)zinc complexes with bulkier *i*Pr groups. Our rationalisation was that, as the alkyl groups essentially coat the surface of the typical (oxido)tetrazinc cluster, an increase in alkyl group bulk should have several desirable influences. First, bulkier alkyl groups should provide better steric protection to inhibit hydrolysis of the interior carbamate linkages by ambient water. Second, they should help to weaken polar interactions between clusters by extending the core-to-core distance. Third, there is evidence that the intrinsic thermal stability of the carbamate group increases with the size of the alkyl group.<sup>[18]</sup>

Our attempts to prepare an (oxido)zinc complex of the sterically bulky *i*Pr<sub>2</sub>NCO<sub>2</sub><sup>-</sup> ligand were not immediately successful.<sup>[19]</sup> Adaptations of previously reported syntheses of (carbamato)tetrazinc complexes such as [Zn<sub>4</sub>(μ<sub>4</sub>-O)(O<sub>2</sub>-CNEt<sub>2</sub>)<sub>6</sub>] proved problematic on several fronts, when applied using the *i*Pr<sub>2</sub>NCO<sub>2</sub><sup>-</sup> ligand. Difficulties included irreproducibility, low yield, and indications that mixtures of several carbamate products were formed. The well-established Cl<sup>-</sup>/*i*Pr<sub>2</sub>NCO<sub>2</sub><sup>-</sup> metathesis process, which was used to prepare similar complexes of other divalent transition metal cations,<sup>[20,21]</sup> proved especially problematic when applied to anhydrous ZnCl<sub>2</sub>. The low reactivity of this material led to incomplete reactions and partially substituted chloride-containing species, confirming previous outcomes with the Et<sub>2</sub>NCO<sub>2</sub><sup>-</sup> ligand.<sup>[22]</sup>

In this paper, the dialkylzinc compound ZnEt<sub>2</sub> is found to be a useful starting material for the self-assembly of tetra- and octanuclear (carbamato)(μ-oxido)zinc clusters from HNR<sub>2</sub>, CO<sub>2</sub> and H<sub>2</sub>O. Specifically, we report the high-yielding and reproducible synthesis (Scheme 1) of the first homonuclear (diisopropylcarbamato)(μ<sub>4</sub>-oxo)zinc complex, [Zn<sub>4</sub>(μ<sub>4</sub>-O)(O<sub>2</sub>CN*i*Pr<sub>2</sub>)<sub>6</sub>] (**1**), and its closely related dimer [Zn<sub>8</sub>(μ<sub>4</sub>-O)<sub>2</sub>(O<sub>2</sub>CN*i*Pr<sub>2</sub>)<sub>12</sub>] (**2**). The new ZnEt<sub>2</sub> method also serves as a more reliable route (Scheme 1) to the known [Zn<sub>4</sub>(μ<sub>4</sub>-O)(O<sub>2</sub>CNEt<sub>2</sub>)<sub>6</sub>] (**3**), and it may prove even more widely applicable.



Scheme 1. Synthetic pathway to prepare (oxido)zinc complexes **1**–**3**. \*Additional recrystallisation step required in resolving these isomers.

X-ray diffraction experiments established the mono-(oxido) [Zn<sub>4</sub>O]<sup>6+</sup> core structure of **1** and **3**, and the bis-(oxido) [Zn<sub>8</sub>O<sub>2</sub>]<sup>12+</sup> core of **2**. The tendency of the *i*Pr<sub>2</sub>NCO<sub>2</sub><sup>-</sup> ligand to form large cluster complexes containing the bis(oxido) core [M<sub>8</sub>O<sub>2</sub>]<sup>12+</sup> is prevalent; however, the mono(oxido) core of **1** is a novel occurrence for this ligand. Moreover, transition between mono- and bis(oxido) cores has been documented for the first time through the experimental interconversion of **1** and **2**. The facility of this interconversion is remarkable as it requires significant reorganisation of Zn–O bonds. The interconversion behaviour outlined in this paper may have a broader significance in considering the solid- and solution-state structures of other polynuclear metallocarbamates.

## Results and Discussion

### Synthesis and Crystal Structures of (Oxido)zinc Complexes **1**–**3**

The initial reaction between ZnEt<sub>2</sub> and HNR<sub>2</sub> (Scheme 1) did not appear to give total conversion to the diamide Zn(NR<sub>2</sub>)<sub>2</sub>, instead reaching equilibrium at the partially substituted intermediate [EtZn(NR<sub>2</sub>)(HNR<sub>2</sub>)] (vide infra), in agreement with previous reports.<sup>[23]</sup> After addition of CO<sub>2</sub>, however, complete substitution of the ethyl groups did occur, presumably by ligand transfer with R<sub>2</sub>NCO<sub>2</sub><sup>-</sup>. The white solids precipitated at this stage were deemed to be polymeric [{Zn(O<sub>2</sub>CNR<sub>2</sub>)<sub>2</sub>]<sub>n</sub>] species due to their insolubility; similar polymeric anhydrous zinc carboxylates have been found in other studies.<sup>[2]</sup>

The subsequent hydrolysis proceeds in a controlled manner, by the insoluble intermediates reacting slowly with a stoichiometric amount of water diluted in THF, to form the benzene-soluble (oxido)zinc complexes (Scheme 1). The solubility of the products makes this step self-indicating to some extent, but it is crucial to allow the hydrolysis reaction to proceed over a further extended period after dissolution to ensure completion of the reaction, otherwise a mixture of carbamate species is recovered upon concentration of the reaction solution. This insight may explain the low yields incurred in previously reported syntheses of complex **3** with the diethylcarbamato ligand.<sup>[8]</sup>

[Zn<sub>4</sub>(μ<sub>4</sub>-O)(O<sub>2</sub>CNEt<sub>2</sub>)<sub>6</sub>] (**3**) was isolated from the HNEt<sub>2</sub> reaction as a fine, free-flowing white powder. Crystals of **3** were grown by slow cooling of a hot heptane solution of the complex (Table 1, Procedure H). Initially, the complex emerged from solution as solventless cubic crystals (space group *I* $\bar{4}3d$ ), but when left in the mother liquor it converted to give an unstable solvent-containing polymorph, possibly the partially characterised tetragonal (*I*<sub>4</sub>*1**a*) form.<sup>[3]</sup> When out of solution, the solventless crystals were stable, and a full set of reflections were collected. The structural data agree with those previously reported for **3**.<sup>[6,8]</sup>

X-ray diffraction studies of the recrystallised HN*i*Pr<sub>2</sub> reaction product provided interesting yet unexpected results. The structure of the (diisopropylcarbamato)(oxido)zinc

Table 1. Recrystallisation parameters for isolated (carbamato)( $\mu$ -oxo)zinc complexes.

Procedure	Starting materials <sup>[a]</sup>	Recrystallisation conditions		Product	
		Solvent	<i>T</i> [°C]	Composition	X-ray
A	crude	CH <sub>3</sub> CN	90	1·2MeCN	full
B	crude	(CH <sub>3</sub> ) <sub>3</sub> CCN	100	1·1.3(CH <sub>3</sub> ) <sub>3</sub> CCN·0.2H <sub>2</sub> O	full
C	crude	C <sub>7</sub> H <sub>16</sub>	110	2·3C <sub>7</sub> H <sub>16</sub> ·3H <sub>2</sub> O	full
D	crude	C <sub>8</sub> H <sub>18</sub>	120	2·3C <sub>8</sub> H <sub>18</sub> ·3H <sub>2</sub> O	full
E	crude	C <sub>14</sub> H <sub>30</sub>	120	2 (solventless)	full
F	1	C <sub>7</sub> H <sub>16</sub>	110	2·C <sub>7</sub> H <sub>16</sub> ·H <sub>2</sub> O	unit cell
G	2	CH <sub>3</sub> CN	90	1·2MeCN	unit cell
H	3	C <sub>7</sub> H <sub>16</sub>	110	3 (solventless)	full

[a] crude: HN*i*Pr<sub>2</sub> reaction product; 1: [Zn<sub>4</sub>( $\mu$ -O)(O<sub>2</sub>CNiPr<sub>2</sub>)<sub>6</sub>], 2: [Zn<sub>8</sub>( $\mu$ -O)(O<sub>2</sub>CNiPr<sub>2</sub>)<sub>12</sub>], 3: [Zn<sub>4</sub>( $\mu$ -O)(O<sub>2</sub>CNEt<sub>2</sub>)<sub>6</sub>].

product was found to vary according to the type of recrystallisation solvent used (Table 1). [Zn<sub>4</sub>( $\mu$ -O)(O<sub>2</sub>CNiPr<sub>2</sub>)<sub>6</sub>] (**1**) was the sole product obtained from CH<sub>3</sub>CN and (CH<sub>3</sub>)<sub>3</sub>CCN recrystallisations (Procedures A and B). The resulting crystals contained varying degrees of lattice solvation and in some cases water, whose origin was most likely adventitious. In its crystal lattices, [Zn<sub>4</sub>( $\mu$ -O)(O<sub>2</sub>CNiPr<sub>2</sub>)<sub>6</sub>] is densely packed, trapping smaller nitrile molecules in the basket-shaped cavities created by surface *i*Pr groups. Vacuum removal of all volatiles left **1** as a white, free-flowing powder; **1** is very sensitive to adventitious moisture, although the stability of the material increased when in crystal form. A high level of solubility was noted in most other organic solvents, including higher nitriles such as propanenitrile, butanenitrile and adiponitrile.

In structural terms, the tetrazinc complex **1** (Figure 1) is a new member of an existing family of basic (carbamato)-zinc complexes, which already includes the dimethyl,<sup>[5]</sup> diethyl,<sup>[3]</sup> dibutyl,<sup>[4]</sup> tetramethylene,<sup>[24]</sup> and pentamethylene<sup>[24]</sup> derivatives. The classic tetrahedral [Zn<sub>4</sub>O]<sup>6+</sup> core of **1** (not explicitly shown) is delimited by Zn–O<sub>oxido</sub> bonds of 1.939 Å average length. The tetrahedron is stabilised by Zn–O<sub>carbamato</sub> bonds ranging from 1.923–1.971 Å in length.

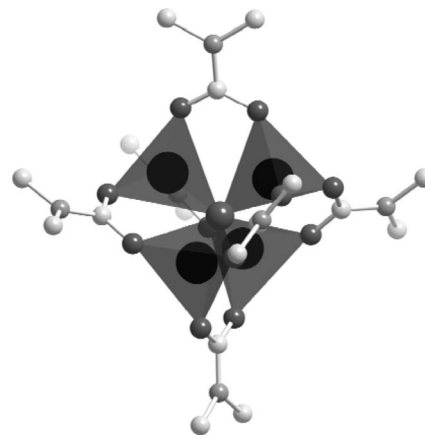


Figure 1. Molecular structure of **1** showing {ZnO<sub>4</sub>} coordination polyhedra. Key: dark tetrahedra = {ZnO<sub>4</sub>}, black circles = Zn, large dark sphere = O<sub>oxido</sub>, small dark spheres = O<sub>carbamato</sub>. Methyl groups and hydrogen atoms are omitted for clarity.

Alternatively, only [Zn<sub>8</sub>( $\mu$ -O)<sub>2</sub>(O<sub>2</sub>CNiPr<sub>2</sub>)<sub>12</sub>] (**2**) was obtained when the HN*i*Pr<sub>2</sub> reaction product was recrystallised from alkanes (Procedures C–E). The octazinc cluster **2** was

Table 2. Crystallographic data for selected compounds.

	1·2CH <sub>3</sub> CN	1·1.3(CH <sub>3</sub> ) <sub>3</sub> CCN·0.2H <sub>2</sub> O	2·3C <sub>7</sub> H <sub>16</sub> ·3H <sub>2</sub> O	2·3C <sub>8</sub> H <sub>16</sub> ·3H <sub>2</sub> O	2	3
Empirical formula	C <sub>42</sub> H <sub>84</sub> N <sub>6</sub> O <sub>13</sub> Zn <sub>4</sub> ·2(C <sub>2</sub> H <sub>5</sub> N)	C <sub>42</sub> H <sub>84</sub> N <sub>6</sub> O <sub>13</sub> Zn <sub>4</sub> ·1.3(C <sub>3</sub> H <sub>9</sub> N)·0.2(H <sub>2</sub> O)	C <sub>84</sub> H <sub>168</sub> N <sub>12</sub> O <sub>26</sub> Zn <sub>8</sub> ·3C <sub>7</sub> H <sub>16</sub> ·3H <sub>2</sub> O	C <sub>84</sub> H <sub>168</sub> N <sub>12</sub> O <sub>26</sub> Zn <sub>8</sub> ·3C <sub>8</sub> H <sub>16</sub> ·3H <sub>2</sub> O	C <sub>84</sub> H <sub>168</sub> N <sub>12</sub> O <sub>26</sub> Zn <sub>8</sub>	C <sub>30</sub> H <sub>60</sub> N <sub>6</sub> O <sub>13</sub> Zn <sub>4</sub>
Formula mass	1224.79	1254.3	2403.5	2682.0	2285.3	974.3
Crystal system	monoclinic	triclinic	trigonal	trigonal	cubic	cubic
Space group	<i>P</i> 2 <sub>1</sub> / <i>c</i>	<i>P</i> $\bar{1}$	<i>R</i> 3	<i>R</i> 3	<i>Pa</i> $\bar{3}$	<i>I</i> $\bar{4}3d$
<i>a</i> [Å]	14.3550(10)	11.574(1)	20.063(2)	19.724(2)	22.594(2)	23.583(2)
<i>b</i> [Å]	35.946(2)	13.728(2)	20.063(2)	19.724(2)	22.594(2)	23.583(2)
<i>c</i> [Å]	24.160(2)	22.950(3)	33.096(9)	33.037(5)	22.594(2)	23.583(2)
$\alpha$ [°]	90	98.004(5)	90	90	90	90
$\beta$ [°]	99.462(1)	101.144(5)	90	90	90	90
$\gamma$ [°]	90	108.253(3)	120	120	90	90
<i>V</i> [Å <sup>3</sup> ]	12297.1	3318.68	11537(4)	11131(2)	11534(2)	13116(1)
<i>Z</i>	8	2	3	3	4	12
<i>D</i> [Mg m <sup>-3</sup> ]	1.323	1.25	1.04	1.20	1.32	1.48
<i>T</i> [K]	150(2)	150(2)	294	150	150(2)	294
Reflections collected	123302	94215	4790	6017	115297	5886
Reflections unique	20574	14228	2892	4585	4249	885
Goodness of fit on <i>F</i> <sup>2</sup>	1.042	1.68	1.46	1.32	0.91	1.33
<i>R</i> <sub>1</sub>	0.0367	0.063	0.053	0.039	0.028	0.044
<i>wR</i> <sub>2</sub>	0.0922	0.088	0.069	0.055	0.039	0.051

also crystallographically identified in crystals grown from  $C_{12}H_{26}$ . Varying degrees of lattice solvation were again noted (Table 2), sometimes including water of crystallisation. The lattice arrangements in  $2 \cdot 3C_7H_{16} \cdot 3H_2O$  and  $2 \cdot 3C_8H_{18} \cdot 3H_2O$  were very similar with molecules of  $[Zn_8(\mu_4-O)_2(O_2CNiPr_2)_{12}]$  regularly spaced between 3-D planes of alternating alkane and  $H_2O$  molecules. Crystals grown from  $C_{14}H_{30}$  contained no solvent. The general physical characteristics of **2** are similar to those observed for **1**.

In a variation on the basic (carbamato)zinc structure, the octazinc complex **2** (Figure 2) essentially consists of two  $[Zn_4O]^{6+}$  cores lashed together by a web of bridging  $iPr_2NCO_2^-$  ligands. As a result of the extended bridging, only two zinc atoms remain in a tetrahedral  $\{ZnO_4\}$  environment. Each of the other zinc atoms is bound in a distorted trigonal-bipyramidal  $\{ZnO_5\}$  coordination. The  $[Zn_8(\mu_4-O)_2(O_2CNiPr_2)_{12}]$  structure belongs to the  $\bar{3}$  symmetry group. Its envelope is an ovoid shape, with an approximate volume of  $3500 \text{ \AA}^3$ . Its bis(oxido)  $[Zn_8O_2]^{12+}$  core (Figure 3) consists of two counterfacing  $[Zn_4O]^{6+}$  tetrahedra aligned on a threefold axis in a staggered fashion. Symmetry rules dictate that two discrete types of zinc atoms exist: Zn1 on the threefold axis, and Zn2. Zn1 is bridged by one type of carbamato ligand to Zn2. The second type of carbamato ligand holds the  $[Zn_8O_2]^{12+}$  core together by binding a Zn2 from each tetrahedron with one oxygen atom (O12), whilst its other oxygen atom (O22) binds a single Zn2. Bond lengths and angles of **2** closely resemble those of previously reported  $[Zn_2Ni_6(\mu_4-O)_2(O_2CNiPr_2)_{12}]$ .<sup>[25]</sup>

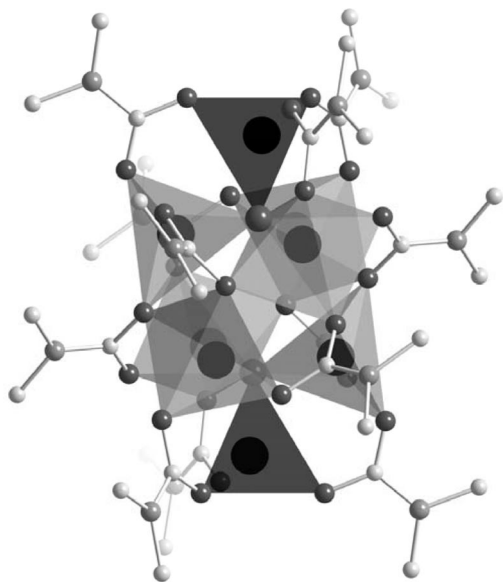


Figure 2. Molecular structure of **2** showing  $\{ZnO_4\}$  and  $\{ZnO_5\}$  coordination polyhedra. Key: dark tetrahedra =  $\{ZnO_4\}$ , light trigonal bipyramids =  $\{ZnO_5\}$ , black circles = Zn, large dark spheres =  $O_{\text{oxido}}$ , small dark spheres =  $O_{\text{carbamato}}$ . Methyl groups and hydrogen atoms are omitted for clarity.

The new octazinc complex **2** matches the  $[M_8(\mu_4-O)_2(O_2CNiPr_2)_{12}]$  structure found for every divalent metal ion along the 4th period, and complexes isostructural with **2** are reported for  $Co^{2+}$ ,  $Fe^{2+}$ ,  $Mn^{2+}$ , and  $Ni^{2+}$ .<sup>[20,21]</sup> The di-

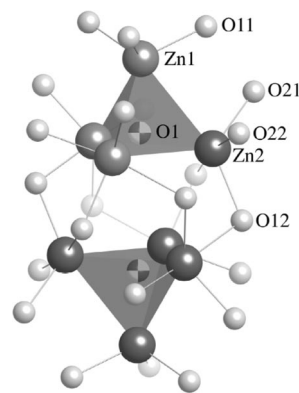
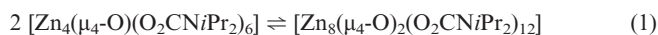


Figure 3. Ball-and-stick model of the core structure of **2**, highlighting  $[Zn_4O]^{6+}$  motifs.  $O^{2-}$  anion represented as patterned sphere. Selected bond lengths [ $\text{\AA}$ ] and angles [ $^\circ$ ]: Zn1–O1 1.958(6), Zn1–O11 1.947(4), Zn2–O1 1.960(1), Zn2–O21 1.976(4), Zn2–O12 2.041(3), Zn2–O12 2.206(4), O1–O1 3.599 (calcd.), Zn2–O22 2.065(4); O1–Zn1–O11 113.9(1), O1–Zn1–O11 113.9(1), O1–Zn1–O11 113.9(1), O11–Zn1–O11 104.7(2), O1–Zn2–O21 115.4(2), O1–Zn2–O12 121.8(2), O1–Zn2–O12 92.0(1), O1–Zn2–O22 96.7(1), O21–Zn2–O12 122.6(2), O21–Zn2–O12 90.2(2), O21–Zn2–O22 91.1(2), O12–Zn2–O12 83.47(7), O12–Zn2–O22 87.2(2), O12–Zn2–O22 169.7(2), Zn2–O12–Zn2 104.67(5), Zn1–O1–Zn2 102.44(6), Zn2–O1–Zn2 115.49(4).

metallic compound  $[Zn_2Ni_6(\mu_4-O)_2(O_2CNiPr_2)_{12}]$  has also been reported, but was obtained only in low yield.<sup>[25]</sup> The structure of  $[Cu_8(\mu_4-O)_2(O_2CNiPr_2)_{12}]$  is somewhat anomalous, it having eight pentacoordinate  $Cu^{2+}$  ions, two of them in square-pyramidal and six in trigonal-bipyramidal configurations.<sup>[26]</sup> This aberration is presumably due to the electronic stabilisation of the  $d^9$  configuration by the square-pyramidal coordination of two  $Cu^{2+}$  ions.

### Interconversion of (Diisopropylcarbamato)(oxido)zinc Complexes

Isolation of crystallographically pure samples of the (carbamato)zinc isomers **1** and **2** allowed the systematic investigation of the isomerisation process. Thus, the tetrazinc complex **1** easily dimerised to give octazinc **2** as the respective solvate, simply by recrystallising it from heptane (Table 1, Procedure F). Likewise, the octazinc complex **2** reverted to its monomeric form when recrystallised from acetonitrile (Procedure G). The combination of these steps is a reversible cycle, the facile interconversion of **1** and **2** [Equation (1)].



Although this type of process has not yet been observed for molecules of the  $[M_4(\mu_4-O)(O_2CNR_2)_6]_x$  type, the fragmentation and recombination of metallocarbamates is not an entirely new concept. The solution dynamics of the hexanuclear complex  $[Co_6(O_2CNET_2)_{12}]$  and its dinuclear dissociation isomer  $[Co_2(O_2CNET_2)_4]$  were studied intensively using UV/Vis techniques, with the result that the lower-nuclearity dinuclear species dominates in solution.<sup>[27]</sup> Despite this dominance, the existence of a facile isomerisation

pathway allowed the deposition of the hexanuclear isomer as the sole solid product. This isomerisation pathway was reported to be necessary to the formation of mixed-metal  $[\text{Co}_x\text{Mg}_{6-x}(\text{O}_2\text{CNET}_2)_{12}]$  complexes.<sup>[27]</sup>

Heterodimetallic carbamate complexes are attractive from a metal oxide film growth perspective. The homonuclear complex  $[\text{Mg}_6(\text{O}_2\text{CNET}_2)_{12}]$  is already a proven precursor for MgO thin-film growth,<sup>[28]</sup> and when mixed with the ( $\mu$ -oxido)zinc analogue  $[\text{Zn}_4(\mu_4\text{-O})(\text{O}_2\text{CNET}_2)_6]$  has been used to deposit dimetallic  $\text{Zn}_x\text{Mg}_{2-x}\text{O}$  films of high quality and reproducibility.<sup>[29]</sup> The next logical step is thus the “mixing” of dimetallic systems at the molecular level, through the formation of a heteronuclear (carbamato)zinc/magnesium complex. Work is currently underway with the diisopropyl series of complexes.<sup>[30]</sup> In a different but related study, Calderazzo et al. reported on future works concerning metal redistribution phenomena for the entire Mn-to-Ni sequence of  $[\text{M}_8(\mu_4\text{-O})_2(\text{O}_2\text{CN}i\text{Pr}_2)_{12}]$  complexes.<sup>[20]</sup> The tetra/octazinc interconversion [Equation (1)] may offer useful insights into those investigating the formation of mixed-metal complexes of the diisopropylcarbamato ligand.

### Solution Analysis of (Oxido)zinc Complexes 1–3

The solution dynamics of diisopropyl complexes **1** and **2** were investigated by  $^1\text{H}$  and  $^{13}\text{C}$  NMR spectroscopy in  $[\text{D}]$ -chloroform,  $[\text{D}_6]$ benzene, and  $[\text{D}_8]$ toluene solvents. A striking observation was made from room-temperature experiments; each complex gave identical solution spectra. This suggested that a common solution species is being formed, a process made possible through the exceptional fluxionality of the complexes. This common species was thought to be the tetrazinc complex  $[\text{Zn}_4(\mu_4\text{-O})(\text{O}_2\text{CN}i\text{Pr}_2)_6]$ , whose symmetry agrees with the characteristically simple ligand spectra we observed (Figure 4, foreground).

However, given the propensity of dialkylcarbamato ligands to exchange when bonded to  $[\text{Zn}_4\text{O}]^{6+}$ ,<sup>[11]</sup> we could

not rule out an analogous exchange environment involving  $[\text{Zn}_8\text{O}_2]^{12+}$  or other intermediates; such a process could also give rise to similar spectral features. Hence, we took to investigating the  $i\text{Pr}_2\text{NCO}_2^-$  ligand environment over a temperature range of 193–368 K. During the course of these experiments, a slight degree of decomposition occurred, as indicated by trace amounts of ZnO powder in the NMR tube and “free”  $\text{HN}i\text{Pr}_2$  appearing in the spectra. This decomposition was slightly accelerated at high temperatures (308–368 K); no other significant spectral changes were observed in this temperature range.

Low-temperature  $^1\text{H}$  NMR studies (Figure 4, inset) revealed a classic case of exchange between inequivalent  $i\text{Pr}$  groups. A  $^{13}\text{C}$  NMR experiment at 193 K (Figure S1) confirmed that the methine carbon resonance had resolved into two broad signals at  $\delta = 47.2$  and 43.9 ppm, while the carboxyl resonance remained sharp and stationary at  $\delta = 161.9$  ppm. The methyl  $^{13}\text{C}$  NMR signals were obscured by solvent peaks and could not be assigned. The chemical shifts of these NMR signals tend towards those of the crystalline-state structure of tetrazinc complex **1**, in which each  $i\text{Pr}_2\text{NCO}_2^-$  ligand clearly presents two inequivalent  $i\text{Pr}$  environments (Figure 5). The variable-temperature NMR results could be explained by a conformational exchange, whereby the  $i\text{Pr}$  groups are projected towards (*endo*) and away (*exo*) from the inner  $[\text{Zn}_4\text{O}]^{6+}$  core of the molecule. While the relatively open structure of **1** accommodates a staggered alkyl conformation (Figure 5), the tightly packed surface of octazinc complex **2** results in only *exo*-oriented  $i\text{Pr}$  groups.

In order to further characterise the solution chemistry of the (diisopropylcarbamato)zinc system, a sample of **2** in THF was analysed using high-resolution ESI-MS. On the positive-ion spectrum, peaks of several di-, tri- and tetranuclear zinc species were detected in the range  $m/z = 850$ –1300 (Figure 6). The tetrazinc complex  $[\text{Zn}_4(\mu_4\text{-O})(\text{O}_2\text{CN}i\text{Pr}_2)_6]$  [ $\text{M}_1$ ] was observed as its proton adduct  $[\text{M}_1 + \text{H}]^+$  at  $m/z$

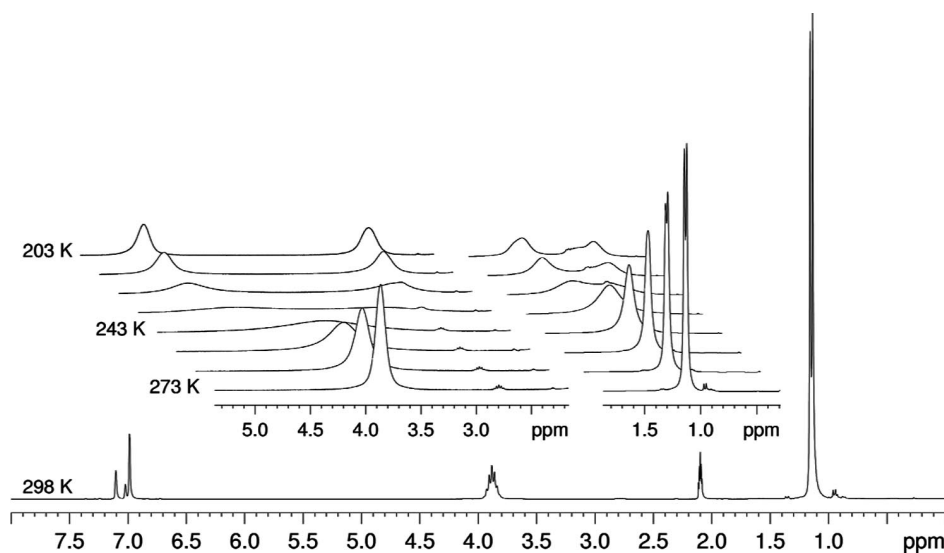


Figure 4. Foreground: room-temperature  $^1\text{H}$  NMR spectrum of **2** in  $[\text{D}_8]$ toluene. Inset: variable-temperature  $^1\text{H}$  NMR stack plot for the same solution.

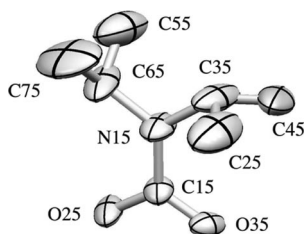


Figure 5. Ellipsoidal diagram of an  $i\text{Pr}_2\text{NCO}_2^-$  ligand from  $\mathbf{1} \cdot 1.3(\text{CH}_3)_3\text{CCN} \cdot 0.2\text{H}_2\text{O}$ . Thermal ellipsoids represent the 30% probability level.

= 1137.3409 and its diisopropylammonium adduct  $[\text{M}_1 + \text{H}_2\text{NiPr}_2]^+$  at  $m/z = 1238.4641$ . Also detected were the fragment ions  $[\text{M}_1 - \text{ZnO} + \text{H}]^+$ ,  $[\text{M}_1 - \text{ZnO} - \text{L}]^+$  and  $[\text{M}_1 - 2\text{ZnO} - \text{L} + 2\text{H}]^+$ , where  $\text{L} = i\text{Pr}_2\text{NCO}_2^-$ . Our interpretations of their structural formulae are provided in Figure 6.

Each peak was computationally simulated utilising the monoisotopic mass, isotopic distribution and background chemistry of the ions in question. As an example, the expanded peak at  $m/z = 1137.3409$  is shown above the corresponding simulation for  $[\text{M}_1 + \text{H}]^+$  in Figure 7. Additional simulation results are given in the Supporting Information (Figures S2–S5). In general, our simulations match the experimental data within 5–11 ppm, which is a reasonable in-

strumental error for the equipment used. Several zinc species of higher nuclearity ( $\text{Zn} > 4$ ) were observed close to the baseline in the mass range  $m/z = 1300\text{--}1800$  (Figure S6), but the low signal-to-noise ratio hampered conclusive identification of those species. No peaks for molecular ions or adduct species were noted for  $[\text{Zn}_8(\mu_4\text{-O})_2(\text{O}_2\text{CN}i\text{Pr}_2)_{12}] [\text{M}_2]$ . On the negative-ion spectrum, a cluster of peaks were also detected close to the baseline at  $m/z = 990\text{--}1050$ , which according to their distributions also appeared to be from tetrazinc species.

The present ESI technique has predominantly detected ionic species of low nuclearity ( $2 \leq \text{Zn} \leq 4$ ), with most peaks exhibiting a degree of protonation. Although this technique did not directly show the concentration of neutral species such as **1** and **2**, we were presented with a rich variety of fragment species, a consequence of the labile chemistry of the system. Other researchers studying the related cobalt complex  $[\text{Co}_8(\mu_4\text{-O})_2(\text{O}_2\text{CN}i\text{Pr}_2)_{12}]$  using DCI-MS reported only octanuclear anions and a singly charged fragment appearing to be  $[\text{Co}_4(\mu_4\text{-O})(\text{O}_2\text{CN}i\text{Pr}_2)_6]^-$ .<sup>[20]</sup> From their data, the observed ratio of octanuclear to tetranuclear ions was 1.8:1. We are continuing to employ other techniques to characterise solution kinetics of the newly discovered diisopropyl derivatives **1** and **2**.  $^1\text{H}$  and  $^{13}\text{C}$  NMR solution spectra of complex **3** agree with literature data.<sup>[6]</sup>

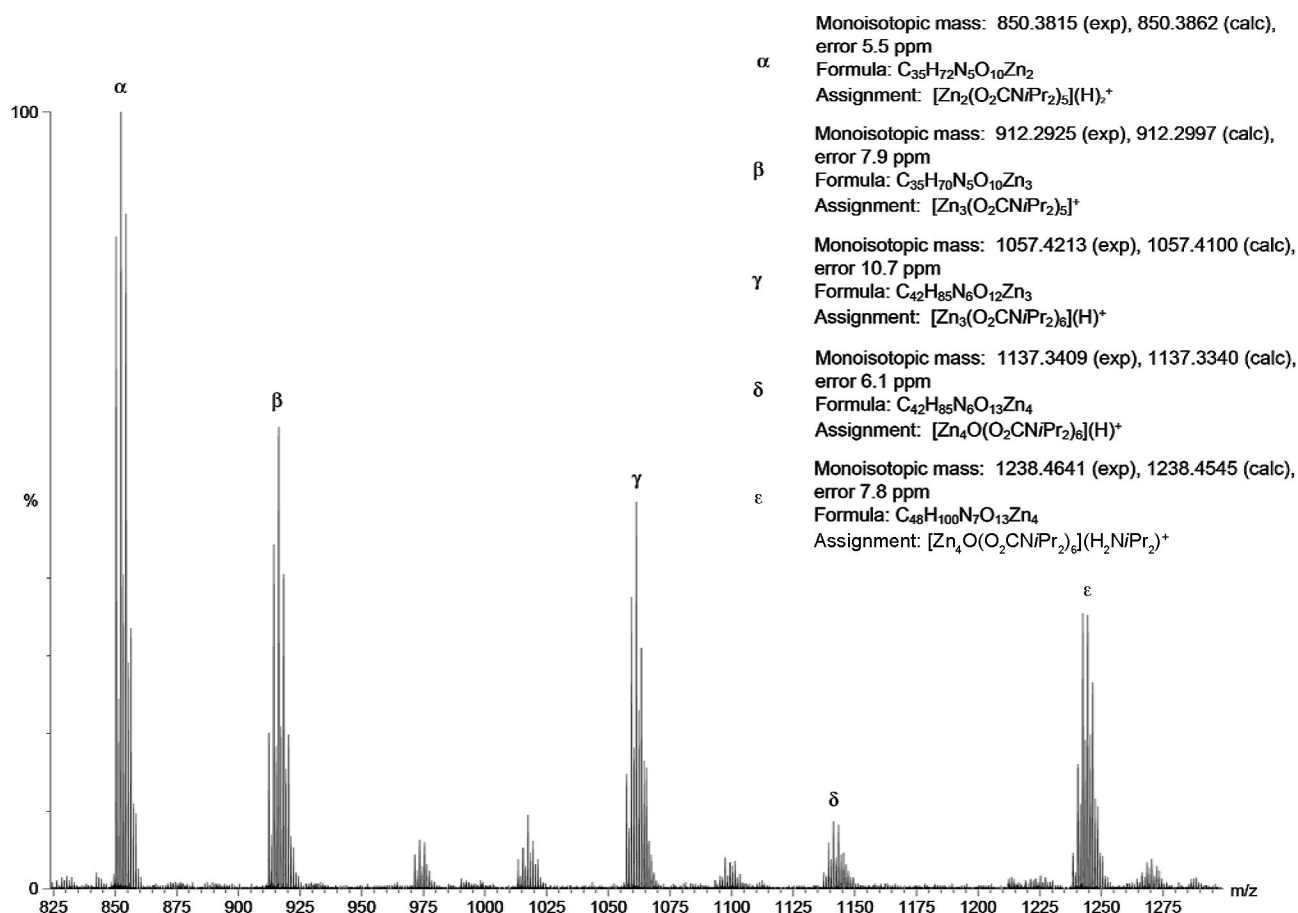


Figure 6. High-resolution positive ion ESI mass spectrum of **2** dissolved in tetrahydrofuran ( $m/z = 825\text{--}1300$ ).

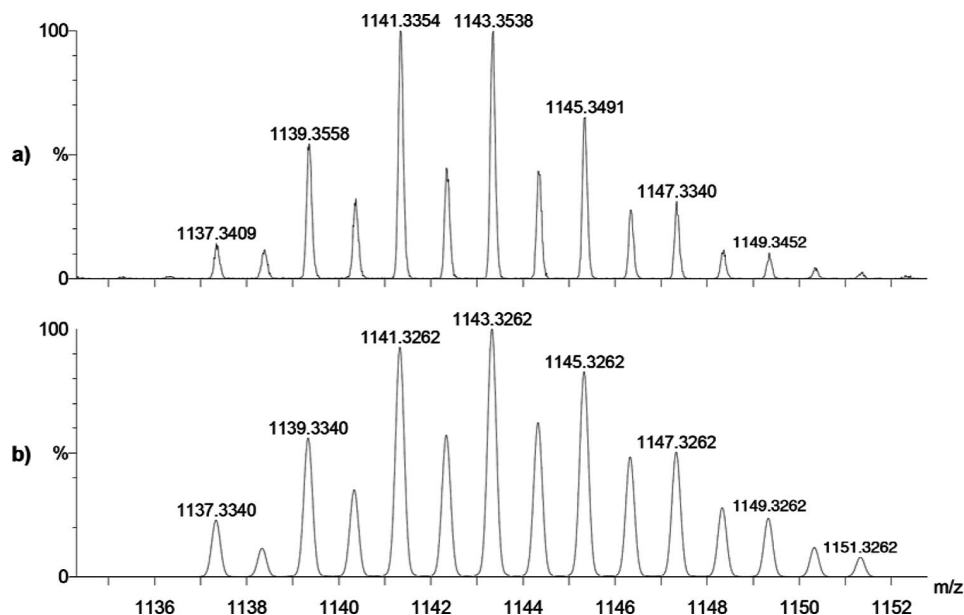


Figure 7. Expanded molecular adduct region for  $[M_1 + H]^+$ , where  $M_1 = [Zn_4(\mu_4-O)(O_2CNiPr_2)_6]$  (**1**). (a) Experimental isotopic distribution; (b) calculated isotopic distribution for  $C_{42}H_{85}N_6O_{13}Zn_4^+$ .

## Conclusion

A convenient new route has been developed for the synthesis of (carbamato)zinc complexes. The (diisopropylcarbamato)( $\mu$ -oxo)zinc complexes participate in an unusually facile isomerisation that allows selective isolation of its tetrazinc or octazinc isomers by choice of recrystallisation solvent. The amount of bond breaking and forming required for the isomerisation between tetrazinc complex **1** and octazinc complex **2** would appear, superficially, to be a significant barrier to the process. However, when the general lability of carbamato ligands<sup>[31]</sup> is appreciated, the tetra/octazinc interconversion finds its place comfortably among other dialkylcarbamato-associated phenomena including metal-centre lability,<sup>[32]</sup> transamination,<sup>[6]</sup> and  $CO_2$  scrambling.<sup>[6]</sup>

The subtle solvent effects discovered in this work may stimulate a re-examination of carbamate chemistry of other metals. In particular, the lability of the (carbamato)zinc complexes offers a route to mixed-metal clusters with possible applications in SSCVD deposition of dimetallic oxide films.

## Experimental Section

**Materials:** Secondary amines were distilled from KOH and stored under argon. Neat  $ZnEt_2$  was purchased from Aldrich and used as received. **Caution:** Diethylzinc is pyrophoric and must be handled with care under an inert gas! Anaerobic-grade  $CO_2$  was obtained from BOC Gases and used without further purification. Acetonitrile, benzene, *n*-heptane and trimethylacetone were dried using standard procedures and stored under argon. Other alkanes were purchased from Aldrich and used as received.  $[D_6]$ Chloroform was purchased from Aldrich and distilled from  $CaH_2$  under argon.  $[D_6]$ -Benzene and  $[D_8]$ toluene were purchased from Aldrich and used

as received. Millipore-grade water was deoxygenated by distillation under argon prior to use. All preparative reactions and product manipulations were carried out under argon using standard Schlenk techniques, unless otherwise specified.

**Instrumentation:**  $^1H$  and  $^{13}C$  NMR spectra were recorded with Bruker DMX 500 and DPX 300 instruments. Mass spectra were recorded with a Q-TOF Ultima API instrument. Ionic distributions were simulated using iMass and MassLynx™ software packages.<sup>[33,34]</sup>

**Synthesis of (Dialkylcarbamato)( $\mu_4$ -oxido)zinc Complexes  $[Zn_4(\mu_4-O)(O_2CNiPr_2)_6]$  (**1**) and  $[Zn_8(\mu_4-O)_2(O_2CNiPr_2)_{12}]$  (**2**):** Under an inert gas, diethylzinc (10.0 mL, 98 mmol) was added to a 250-mL 3-necked flask fitted with a reflux condenser. Benzene (100 mL) and diisopropylamine (28.0 mL, 200 mmol) were added to the flask, and the mixture was refluxed for 2 h, with evolution of a colourless gas and formation of an olive coloured solution. The cooled solution was exposed to a stream of  $CO_2$  overnight to form a cloudy grey mixture. A further aliquot of benzene was then added (70 mL), then the mixture was cooled to 0 °C, and  $H_2O$  (440  $\mu$ L, 24 mmol) in dried THF (20 mL) introduced dropwise with vigorous stirring under  $CO_2$ . No immediate change was evident but, after 24 h, a clear solution resulted. All volatiles were removed in vacuo leaving a white powder (28 g, ca. quant. yield based on Zn in  $ZnEt_2$ ). Recrystallisation from  $CH_3CN$  and  $(CH_3)_3CN$  gave **1** as a crystalline solvate, while recrystallisation from  $C_7$ – $C_{14}$  alkanes gave **2** (see Table 1). **1:**  $^1H$  NMR (300 MHz,  $CDCl_3$ ):  $\delta$  = 1.19 (d, 12 H,  $CH_3$ ), 3.91 (sept, 2 H, CH) ppm.  $^{13}C$  NMR (76.6 MHz,  $CDCl_3$ ):  $\delta$  = 162.0 ( $CO_2$ ), 45.64 (CH), 20.80 ( $CH_3$ ) ppm.  $C_{42}H_{85}N_6O_{13}Zn_4$  (1142.7): calcd. C 44.15, H 7.41, N 7.35; found C 44.05, H 7.41, N 7.34. **2:**  $C_{84}H_{168}N_{12}O_{26}Zn_8$  (2285.4): calcd. C 44.15, H 7.41, N 7.35; found C 44.28, H 7.52, N 7.37.

**$[Zn_4(\mu_4-O)(O_2CNEt_2)_6]$  (**3**):** Diethylamine (16.8 mL, 160 mmol) was added to a solution of diethylzinc (8.2 mL, 80 mmol) in benzene (100 mL) in a 250-mL three-necked flask fitted with a reflux condenser under an inert gas. The resulting clear solution was heated under reflux for 2 h, during which the solution became yel-

low, with concomitant evolution of a colourless gas. The solution was cooled, then stirred whilst a stream of CO<sub>2</sub> gas was passed over it overnight, to give a white cloudy mixture. After cooling to 0 °C, a solution of H<sub>2</sub>O (300 μL, 17 mmol) in THF (30 mL) was added dropwise to the stirred mixture, leading to an increase in turbidity. After stirring at room temperature for 48 h, the mixture had become a clear solution. Volatiles were removed under reduced pressure to give a white solid. The tetranuclear complex **3** was isolated as a white powder (16.8 g, 86%) by recrystallisation of the solid from hot heptane and subsequent removal of solvent under reduced pressure. <sup>1</sup>H NMR (300 MHz, CDCl<sub>3</sub>): δ = 1.08 (t, 6 H, CH<sub>3</sub>), 3.27 (q, 4 H, CH<sub>2</sub>) ppm. <sup>13</sup>C NMR (76.6 MHz, CDCl<sub>3</sub>): δ = 162.4 (CO<sub>2</sub>), 41.54 (CH<sub>2</sub>), 13.58 (CH<sub>3</sub>) ppm.

### X-ray Crystallography

**Recrystallisation Procedure:** The experimental setup consisted of a B-type bushing 38-mL heavy-walled glass pressure tube (Ace Glass) containing stirrer bar and recrystallisation materials under argon. A volume of 10 mL of solvent per gram of (diisopropylcarbamato)-zinc complex was found to give crystals of adequate quality. For **1**·2CH<sub>3</sub>CN, a sealed vial containing **1** or **2** and CH<sub>3</sub>CN was heated and stirred up to 90 °C, the white powder dissolving to give a colourless solution. Heating was ceased, and the tube was cooled slowly at the cooling rate of the bath; 24 h later a crop of colourless rectangular-prism-shaped crystals (**1**·2CH<sub>3</sub>CN) was collected. For **2**·3C<sub>7</sub>H<sub>16</sub>·3H<sub>2</sub>O, similarly, a 110 °C hot solution of **1** or **2** in C<sub>7</sub>H<sub>16</sub> was cooled to give rhomboid-shaped crystals (**2**·3C<sub>7</sub>H<sub>16</sub>·3H<sub>2</sub>O). Other procedures (Table 1) followed in a similar manner.

**Structure Determination:** Reflection data were measured with an Enraf–Nonius CAD-4 diffractometer in the  $\theta/2\theta$ -scan mode using graphite-monochromatized molybdenum radiation ( $\lambda = 0.71073$  Å). Data were corrected for absorption using the analytical method of de Meulenaer and Tompa.<sup>[35]</sup> Reflections with  $I > 2\sigma(I)$  were considered observed. Structures were determined by direct phasing and Fourier methods. Hydrogen atoms were included in calculated positions and were assigned thermal parameters equal to those of the atom to which they were bonded. Positional and anisotropic thermal parameters for the non-hydrogen atoms were refined using full-matrix least squares. Reflection weights used were  $1/s^2(F_o)$ , with  $s(F_o)$  being derived from  $s(I_o) = [s^2(I_o) + (0.04I_o)^2]^{1/2}$ . The weighted residual is defined as  $R_w = (S w D^2 / S w F_o^2)^{1/2}$ . Atomic scattering factors and anomalous dispersion parameters were from the International Tables for X-ray Crystallography.<sup>[36]</sup> The structure solution was done with SIR92<sup>[37]</sup> and the refinement with RAELS.<sup>[38]</sup> ORTEP-II<sup>[39]</sup> for eMac was used for the structural diagrams, and an eMac was used for the calculations. CCDC-653246 (**2**), -653247 [**1**·1.3(CH<sub>3</sub>)<sub>3</sub>CCN·0.2H<sub>2</sub>O], -653248 (**2**·3C<sub>7</sub>H<sub>16</sub>·3H<sub>2</sub>O), -653249 (**3**), -658301 (**1**·2CH<sub>3</sub>CN) and -676333 (**2**·C<sub>8</sub>H<sub>18</sub>) contain the supplementary crystallographic data for this paper. These data can be obtained free of charge from The Cambridge Crystallographic Data Centre via [www.ccdc.cam.ac.uk/data\\_request/cif](http://www.ccdc.cam.ac.uk/data_request/cif).

**Supporting Information** (see footnote on the first page of this article): Additional mass spectrometric and NMR spectroscopic data (Figures S1–S6).

### Acknowledgments

The authors wish to thank Paul Jensen from the Crystal Structure Analysis Facility at Sydney University for low-temperature single-crystal X-ray data collection. The authors are also very grateful to staff at the UNSW Analytical Centre's NMR facility for assistance with variable-temperature NMR spectroscopy experiments and the

Bioanalytical Mass Spectrometry Facility (BMSF) for conducting ESI-MS experiments.

- [1] O. Berkesi, I. Dreveni, A. Andor, *Inorg. Chim. Acta* **1991**, *181*, 285–289; J. Charalambous, R. G. Copperthwaite, W. Jeffs, D. E. Shaw, *Inorg. Chim. Acta* **1975**, *14*, 53–58; R. M. Gordon, H. B. Silver, *Can. J. Chem.* **1983**, *61*, 1218; H. Koyama, Y. Saito, *Bull. Chem. Soc. Jpn.* **1954**, *27*, 112–114.
- [2] W. Clegg, D. R. Harbron, C. D. Homan, P. A. Hunt, I. R. Little, B. P. Straughan, *Inorg. Chim. Acta* **1991**, *186*, 51–60.
- [3] A. Belforte, F. Calderazzo, U. Englert, J. Straehle, *Inorg. Chem.* **1991**, *30*, 3778–3781.
- [4] D. B. Dell'Amico, F. Calderazzo, S. Farnocchi, L. Labella, F. Marchetti, *Inorg. Chem. Commun.* **2002**, *5*, 848–852.
- [5] D. B. Dell'Amico, F. Calderazzo, L. Labella, F. Marchetti, *Inorg. Chim. Acta* **2003**, *350*, 661–664.
- [6] C. S. McCowan, L. G. Thomas, M. T. Caudle, *Inorg. Chem.* **2002**, *41*, 1120–1127.
- [7] R. Murugavel, M. Saythivendiran, M. G. Walawalkar, *Inorg. Chem.* **2001**, *40*, 427–434.
- [8] M. A. Malik, P. O'Brien, M. Motevalli, I. Abrahams, *Polyhedron* **2006**, *25*, 241–250.
- [9] S. C. Abrahams, J. L. Bernstein, *Acta Crystallogr., Sect. B* **1969**, *25*, 1233–1236; T. M. Sabine, S. Hogg, *Acta Crystallogr., Sect. B* **1969**, *25*, 2254–2256.
- [10] M. Casarin, E. Tondello, F. Calderazzo, A. Vittadini, M. Bettinelli, A. Gulino, *J. Chem. Soc. Faraday Trans.* **1993**, *89*, 4363–4367.
- [11] C. S. McCowan, M. T. Caudle, *Dalton Trans.* **2005**, 238–246.
- [12] A. J. Petrella, H. Deng, N. K. Roberts, R. N. Lamb, *Chem. Mater.* **2002**, *14*, 4339–4342.
- [13] G. L. Mar, P. Y. Timbrell, R. N. Lamb, *Chem. Mater.* **1995**, *7*, 1890–1896.
- [14] M. H. Koch, A. J. Hartmann, R. N. Lamb, M. Neuber, J. Walz, M. Grunze, *Surf. Rev. Lett.* **1997**, *4*, 39–44; N. H. Tran, A. J. Hartmann, R. N. Lamb, *J. Phys. Chem. B* **1999**, *103*, 4264–4268.
- [15] M. R. Hill, A. W. Jones, J. J. Russell, N. K. Roberts, R. N. Lamb, *Inorg. Chim. Acta* **2005**, *358*, 201–206.
- [16] M. H. Koch, A. J. Hartmann, R. N. Lamb, M. Neuber, M. Grunze, *J. Phys. Chem. B* **1997**, *101*, 8231–8236.
- [17] D. B. Dell'Amico, F. Calderazzo, F. Marchetti, G. Pampaloni, *NATO ASI Ser., Ser. 3* **1995**, *5*, 199–209.
- [18] U. P. Kreher, A. E. Rosamilia, C. L. Raston, J. L. Scott, C. R. Strauss, *Molecules* **2004**, *9*, 387–393.
- [19] P. F. Haywood, Honours Thesis, UNSW, **2005**.
- [20] D. Belli Dell'Amico, C. Bradicich, F. Calderazzo, A. Guarini, L. Labella, F. Marchetti, A. Tomei, *Inorg. Chem.* **2002**, *41*, 2814–2816.
- [21] D. B. Dell'Amico, F. Calderazzo, L. Labella, C. Maichle-Moessmer, J. Straehle, *J. Chem. Soc., Chem. Commun.* **1994**, 1555–1556.
- [22] C. S. McCowan, C. E. Buss, V. G. Young Jr, R. L. McDonnell, M. T. Caudle, *Acta Crystallogr., Sect. E* **2004**, *60*, m285–m287.
- [23] M. A. Malik, P. O'Brien, *Polyhedron* **1997**, *16*, 3593–3599.
- [24] C. S. McCowan, T. L. Groy, M. T. Caudle, *Inorg. Chem.* **2002**, *41*, 1120–1127.
- [25] A. Bacchi, D. B. Dell'Amico, F. Calderazzo, U. Giurlani, G. Pelizzi, L. Rocchi, *Gazz. Chim. Ital.* **1992**, *122*, 429–435.
- [26] F. Calderazzo, D. B. Dell'Amico, G. Pelizzi, *Gazz. Chim. Ital.* **1985**, *115*, 145–146.
- [27] M. T. Caudle, J. B. Benedict, C. K. Mobley, N. A. Straessler, T. L. Groy, *Inorg. Chem.* **2002**, *41*, 3183–3190.
- [28] M. R. Hill, A. W. Jones, J. J. Russell, N. K. Roberts, R. N. Lamb, *J. Mater. Chem.* **2004**, *14*, 3198–3202.
- [29] M. R. Hill, J. J. Russell, R. N. Lamb, *Chem. Mater.*, in press.
- [30] M. R. Hill, J. J. Russell, P. Jensen, R. N. Lamb, *Dalton Trans.*, in press.
- [31] D. B. Dell'Amico, F. Calderazzo, L. Labella, F. Marchetti, M. Martini, I. Mazzoncin, *C. R. Chim.* **2004**, *7*, 877–884.

- [32] M. T. Caudle, B. B. Jason, K. M. Charles, A. S. Nicholas, L. G. Thomas, *Inorg. Chem.* **2002**, *41*, 3183–3190.
- [33] U. Röthlisberger, *iMass*, **2002**.
- [34] *MassLynx*<sup>TM</sup>, Waters Corporation, Massachusetts, **2002**.
- [35] J. de Meulenaer, H. Tompa, *Acta Crystallogr.* **1965**, *19*, 1014–1018.
- [36] *International Tables for X-ray Crystallography* (Eds: J. A. Ibers, W. C. Hamilton), Kynoch Press, Birmingham, **1974**, vol. 4.
- [37] A. Altomare, M. C. Burla, M. Camalli, G. Cascarano, C. Giacovazzo, A. Guagliardi, G. Polidori, *J. Appl. Crystallogr.* **1994**, *27*, 1045–1050.
- [38] A. D. Rae, *RAELS*, University of New South Wales, Sydney, **1996**.
- [39] C. K. Johnson, *ORTEP-II*, Oak Ridge National Laboratory, Tennessee, **1976**.

Received: July 12, 2007

Published Online: March 13, 2008

(Since its publication in Early View, a few minor changes have been made.)